Journal of Visualized Experiments

Sample Preparation by 3D-Correlative Focused Ion Beam Milling for High-Resolution Cryo-Electron Tomography.

--Manuscript Draft--

Article Type:	Invited Methods Collection - JoVE Produced Video
Manuscript Number:	JoVE62886R1
Full Title:	Sample Preparation by 3D-Correlative Focused Ion Beam Milling for High-Resolution Cryo-Electron Tomography.
Corresponding Author:	Philipp Erdmann Fondazione Human Technopole Milan, Lombardy ITALY
Corresponding Author's Institution:	Fondazione Human Technopole
Corresponding Author E-Mail:	philipp.erdmann@fht.org
Order of Authors:	Anna Bieber
	Cristina Capitanio
	Florian Wilfling
	Jürgen Plitzko
	Philipp Erdmann
Additional Information:	
Question	**Response**
Please specify the section of the submitted manuscript.	Biology
Please indicate whether this article will be Standard Access or Open Access.	Open Access ($3900)
Please indicate the **city, state/province, and country** where this article will be **filmed**. Please do not use abbreviations.	Munich, Bavaria, Germany
Please confirm that you have read and agree to the terms and conditions of the author license agreement that applies below:	I agree to the Author License Agreement
Please provide any comments to the journal here.	
Please confirm that you have read and agree to the terms and conditions of the video release that applies below:	I agree to the Video Release

TITLE:

Sample Preparation by 3D-Correlative Focused Ion Beam Milling for High-Resolution Cryo-Electron Tomography

AUTHORS AND AFFILIATIONS:

Anna Bieber[1*], Cristina Capitanio[1*], Florian Wilfling[1,2], Jürgen Plitzko[1#], Philipp S. Erdmann[1,3#]

[1]Max Planck Institute of Biochemistry, Martinsried, Germany
[2]Max Planck Institute for Biophysics, Frankfurt, Germany
[3]Fondazione Human Technopole, Milan, Italy

*These authors contributed equally.

Email addresses of co-authors:
Anna Bieber (anbieber@biochem.mpg.de)
Cristina Capitanio (capitanio@biochem.mpg.de)
Florian Wilfling (florian.wilfling@biophys.mpg.de)
Jürgen Plitzko (plitzko@biochem.mpg.de)
Philipp S. Erdmann (philipp.erdmann@fht.org)

#Corresponding authors:
Jürgen Plitzko (plitzko@biochem.mpg.de)
Philipp S. Erdmann (philipp.erdmann@fht.org)

KEYWORDS:

cryo-electron tomography, cryo-focused ion beam milling, *in situ* structural biology

SUMMARY:

Here, we present a pipeline for 3D-correlative focused ion beam milling on guiding the preparation of cellular samples for cryo-electron tomography. The 3D position of fluorescently tagged proteins of interest is first determined by cryo-fluorescence microscopy, and then targeted for milling. The protocol is suitable for mammalian, yeast, and bacterial cells.

ABSTRACT:

Cryo-electron tomography (cryo-ET) has become the method of choice for investigating cellular ultrastructure and molecular complexes in their native, frozen-hydrated state. However, cryo-ET requires that samples are thin enough to not scatter or block the incident electron beam. For thick cellular samples, this can be achieved by cryo-focused ion beam (FIB) milling. This protocol describes how to target specific cellular sites during FIB milling using a 3D-correlative approach, which combines three-dimensional fluorescence microscopy data with information from the FIB-scanning electron microscope. Using this technique, rare cellular events and structures can be targeted with high accuracy and visualized at molecular resolution using cryo-transmission electron microscopy (cryo-TEM).

INTRODUCTION:

Focused ion beam milling allows the preparation of thin biological samples from cryo-fixed specimens without the problems commonly associated with mechanical sectionings such as knife marks and compression artifacts[1]. When paired with cryo-electron tomography, FIB milling enables high-resolution biological studies of the cellular morphology and determination of the structure of macromolecular complexes directly from within cells at sub-nanometer resolution[2–4]. While abundant species, such as ribosomes, are readily found in randomly cut FIB lamellas, many cellular processes rely on the colocalization of several complexes or are localized to specific sites within the cell. Consequently, efficient targeting is required to not lose the biological feature of interest during the milling process and be limited to random hits. A correlative approach that combines data from the scanning electron microscope (SEM)-FIB and a cryo-fluorescence light microscope (FLM) is therefore necessary. While it is possible to omit the initial correlation and combine FLM and cryo-ET data only after TEM acquisition[5,6], fluorescence-guided focused ion beam milling enables an accurate selection of the milling area beforehand, thereby resulting in more efficient data acquisition. Since its conception[7], the application of 3D-correlated FIB milling in biological studies had been limited until we recently reported identifying a new liquid-liquid phase-separated (LLPS) compartment in yeast using this technique[8].

Described here is a generalized 3D cryo-correlated light and electron microscopy (CLEM) protocol, which can be used to study a broad variety of samples ranging from bacteria to yeast and mammalian cells. While the experiments were performed using a certain set of instruments, the individual steps are not bound to specific hardware and can easily be transferred to other systems as an extension to existing protocols[3,5]. A list of tested equipment and suggested settings are provided in the **Table of Materials** and **Table 1**. The four key steps of the pipeline are (1) sample preparation, (2) localization of features of interest by cryo-fluorescence microscopy, (3) 3D-correlated focused ion beam milling, and (4) localization of the targeted structures for cryo-ET data acquisition on the lamellas in the cryo-transmission electron microscope (**Figure 1**).

PROTOCOL:

[Place **Figure 1** here]

1. Cell culture and plunge freezing of grids

1.1. Culture cells of choice and optimize labeling and treatment strategies at room temperature before moving to cryo-experiments. Targets of interest are either labeled using fluorescent protein fusions or live staining (e.g., Halo-Tag, LysoTracker, BODIPY, live antibody staining, etc.). If treatment with chemical or biological agents (small molecules, special media, siRNA, etc.) is needed to investigate the biological process of interest, optimize the conditions (e.g., time, concentration) using live-cell FLM imaging.

1.1.1. Ensure that the sites of interest can be localized successfully above background in a sufficient number of cells using imaging settings that match later cryo-conditions as closely as possible (i.e., NA, exposure time, etc.).

1.2. Selection and preparation of grids

1.2.1. Select grids with hole size and spacing appropriate for the cells and the fiducial markers used (see step 1.3.1). Do not use continuous film without holes as this might result in too much residual buffer after blotting and thus reduce vitrification efficiency and hamper the detection of fiducial beads. For prolonged contact of the cells with the grids, ensure that the grid support and film material are biocompatible.

1.2.2. Plasma-clean the cryo-EM grids to make them more hydrophilic. For use in adherent cell culture, sterilize the grids after plasma-cleaning with UV radiation for 20 min in a laminar flow hood. Optionally, grids may be pre-treated with compounds that help with cell adhesion, such as poly-L-lysine or concanavalin A, as described below.

NOTE: In general, the following grid/sample combinations have successfully been used in the correlative cryo-FIB workflow: Yeast: Cu or Au, 200 mesh, R1/4 carbon or SiO_2 film, optionally coated with concanavalin A; *Escherichia coli*.: Cu or Au, 200 mesh, R1/4 carbon or SiO_2 film; *Chlamydomonas reinhardtii*: Cu or Au, 200 mesh, R1/2 or R1/4 carbon or SiO_2 film; HeLa: Au, 200 mesh, R1/4 SiO_2 film, coated with poly-L-lysine; HEK293: Au, 200 mesh, R1/4 SiO_2 film, coated with poly-L-lysine.

1.2.3. Concanavalin A coating to improve the attachment of yeast cells:

1.2.3.1. Prepare a coating solution of 1 mg/mL of concanavalin A in 10 mM HEPES buffer with 100 µM $CaCl_2$, pH 8.5. Place one drop (50 µL) of the coating solution and two drops of distilled water separately on a piece of paraffin film.

1.2.3.2. Pick up the plasma-cleaned grid with reverse-force tweezers and insert it carefully into the drop of the coating solution, avoiding movements perpendicular to the grid to prevent damage to the film.

1.2.2.3. After ~5 s incubation, wash the grid two times by inserting it into the drops of water in a similar fashion. Finally, blot off the excess liquid by applying a filter paper to the back of the grid and let the grid dry completely before releasing it from the tweezers. Use the dried grids for plunge-freezing.

1.2.4. Poly-L-lysine coating for suspension culture and adherent cells: Prepare a coating solution of 1 mg/mL of poly-L-lysine in 0.1 M sodium borate buffer, pH 8.5. Place plasma-cleaned grids into a suitable dish for cell culture and sterilize for 20 min by UV radiation. Gently add enough coating solution to cover all the grids and incubate at 37 °C for at least 2 h. Aspirate the liquid and gently wash the grids two times with PBS before seeding the cells to the desired concentration.

1.3. Preparation of cells and fiducial beads.

NOTE: Fiducial beads are required for 3D registration of the fluorescence data with images taken in the FIB/SEM microscope to allow 3D-correlative FIB milling.

1.3.1. Choose the beads recognizable in all imaging modalities, i.e., FLM, SEM, and IB (recommended diameter 0.5–1 µm), but ensure these do not outshine the cellular target structure during fluorescence imaging to make it easier to differentiate the beads and the biological feature of interest. Remove cytotoxic preservatives in fiducial beads (e.g., NaN_3) as instructed by the manufacturer.

NOTE: For an easier distinction between the biological features of interest and the fiducials, it is useful if fluorescence emission spectra only partially overlap so that signals can be distinguished based on intensity differences in the FLM channels.

1.3.2. If suspension culture is used, grow the cells to a suitable density (e.g., yeast OD_{600} = 0.8, *E. coli* OD_{600} = 0.8–1.0, *C. reinhardtii* 1500 cells/µL) and perform treatments as required for the experiment such as change of medium, addition of chemicals, starvation, etc. Attach the plasma-cleaned grids to tweezers as required for the plunging method (manual/automatic), and apply 4 µL of the cell suspension mixed with ~1 x 10^5 beads/µL of fiducial bead suspension to the film side of the grids.

NOTE: Determine the optimal dilution of cells and fiducials in titration experiments (e.g., by checking on the cryo-FLM or FIB/SEM, see below). However, for most cells grown in suspension, a final concentration of ~1 x 10^5 beads/µL of the 1 µm fiducial beads (1:20 dilution from stock; see **Table of Materials** for details) has proven a good starting point.

1.3.3. If adherent culture is used, plasma-clean and sterilize the grids using UV-radiation for aseptic culture. If necessary, pre-coat grids with compounds that help cell adhesion (e.g., poly-L-lysine, fibronectin, laminin; see step 1.2.2). Seed and grow cells on the grids in normal culture dishes or dishes with subdivisions for grids.

1.3.4. Treat the samples as necessary for the experiment and maintain the cells in optimal conditions just until plunge freezing (e.g., 37 °C/5% CO_2 for HEK/HeLa). Carefully remove the grids from the culture dish and attach them to the plunging tweezers. Apply 4 µL of the culture medium mixed with fiducials (1 x 10^5 beads/µL for 1 µm fiducials) to the cell-bearing side.

1.4. Plunge-freeze the cells using either a manual or an automated freezing procedure. If possible, only blot the grid from the side opposite to the cells to prevent mechanically damaging the cells (**Figure 2A**). On two-armed automated plunging systems, achieve this by placing a Polytetrafluoroethylene (e.g., Teflon) sheet instead of blotting paper on the pad facing the cells. Transfer the grids to storage boxes and keep them in liquid nitrogen (lN_2) until use.

CAUTION: lN_2 and other cryogens can cause severe damage to the eyes and skin. Use personal protective equipment (PPE) and only work in a well-ventilated space to avoid the buildup of

dangerous N_2 concentrations.

NOTE: All subsequent steps should best be carried out in the liquid phase of lN_2 to avoid contamination of the cell and lamella surfaces, as this might complicate downstream processing. Reduce contact with floating ice crystals by always using clean liquid nitrogen (e.g., filter to remove floating ice), eliminating unnecessary transfer steps, and, if possible, working in a humidity-controlled environment.

1.5. Mount and clip the plunge-frozen grids in AutoGrids with cutout and the cells facing up (**Figure 2A**) for subsequent cryo-fluorescence imaging and FIB milling. To ensure proper alignment of the samples in the TEM, the milling direction needs to be orthogonal to the cryo-ET tilt axis. Accordingly, place the orientation marks (e.g., LASER-engraving or removable marker dots) on AutoGrids before clipping to help with this alignment (**Figure 2A**).

1.6. Screen the grid quality (**Figure 2B**) on the cryo-FLM and FIB/SEM. Optimize the cell density, blotting time, and force to get an even distribution of cells and beads. Use reflected light imaging on a cryo-fluorescence microscope to do this relatively or use the cryo-FIB-SEM to make sure that both cells and fiducial beads are clearly visible (**Figure 2B**, white arrows).

1.7. If necessary, repeat plunging with better conditions, e.g., varying cell concentration and/or blotting time. Once suitable plunging parameters have been found, do not repeat grid screening for each new round of experiments.

[Place **Figure 2** here]

2. Cryo-fluorescence light microscopy

2.1. For each grid, acquire an overview in (widefield) fluorescence and differential interference contrast (DIC) or reflected mode and select suitable grid squares with fluorescence signal. Choose fields of view that contain both the cells of interest and a sufficient number of fiducial markers (6–12).

2.1.1. Ensure that the cells and beads are evenly distributed, not too dense, and toward the center of each square. Only choose the squares accessible both to the FIB-SEM and TEM instrument, hence those at least three squares away from the grid edge on 200 mesh grids (**Figure 3A**, inside the red circle).

2.2. On each of the selected grid squares, acquire a fluorescent stack with a focus step appropriate for later deconvolution, i.e., <½ the axial resolution limit. If possible, use high-numerical-aperture (NA) objectives to increase photon count and localization accuracy.

2.2.1. In a confocal microscope with NA 0.9 objective, acquire stacks with 300 nm step size, oversampling the Nyquist value. Record multiple color stacks if needed (**Figure 2B**). Store grids under lN_2 until further use.

NOTE: To determine the optimal step size, choose the values calculated by the microscope control software or use online tools[9]. Check for bleed-through of signal between channels since excessive bleed-through is detrimental for colocalization experiments. However, some may be advantageous to correct for chromatic aberrations in multi-color stacks.

2.3. Deconvolve stacks using appropriate software[10,11] and re-slice[7] them if the isotropic pixel size is required. Deconvolution—just as at room temperature—cleans up the FLM signal and may improve localization accuracy (**Figure 3C**).

[Place **Figure 3** here]

3. Focused ion beam milling

3.1. Load the grids into the cryo-FIB-SEM instrument and use either the cutout and/or orientation marks to ensure proper orientation for later placement into the TEM (**Figure 2A**). Ensure that the milling direction is perpendicular to the tilt axis of the TEM.

3.2. Use a gas injection system (GIS; $CpMePtMe_3$) at the stage positions pre-defined by the FIB-SEM setup to coat the grids with a protective organometallic layer. Do not apply too much, as this might interfere with fiducial bead localization in the TEM later. Use a plasma coater to apply metallic platinum to reduce sample charging.

NOTE: If no settings for GIS coating are available, they can easily be found by performing successive rounds of short coating (~2 s), followed by FIB milling. Ensure that the sample can still be cut successfully at medium currents (~100 pA) without apparent fringing of the protective organometallic layer around the lamella edges. Both time and distance of the GIS needle (with respect to the sample) are important parameters to consider. Do not operate the GIS needle at room-temperature settings (i.e., 45 °C), but as cold as possible to still provide an even coating (25–27 °C).

3.3. Record the SEM grid overview and perform a 2D correlation with FLM overviews to find the grid squares for which fluorescent stacks have been recorded. Manually inspect both views or use various software packages[7,10,12] to find the grid squares. Here, the focus is on the 3D correlation toolbox (3DCT)[7], which uses 3D rigid body transformation with isotropic scaling between views. An excellent walk-through on 3DCTs functions is available online[13].

3.3.1. Select and mark at least four corresponding positions, e.g., landmarks such as grid bars or holes in the support film, in both the FLM and SEM grid overview (right-click) and calculate the transformation between the marked points (correlate).

3.3.2. Next, place the markers in the center of the corresponding grid squares for which FLM stacks have been acquired and predict their position in the SEM view (correlate; **Figure 4A**).

3.4. For each correlated grid square, take a low-current (≤10 pA) ion beam (IB) image at the FIB milling angle of choice (10°–25° for 45° pre-tilt shuttle). Select a field of view (i.e., position and magnification) that matches the fluorescence data. For 200 mesh grids, acquire fluorescence and FIB/SEM data to contain single grid squares, including the grid bars (see **Figure 3A** and **Figure 4A**).

NOTE: Milling should be performed at as shallow an angle as possible to avoid losing significant angular range during cryo-ET and allowing identification of a sufficient number of fiducial beads. For example: with a stage tilt of 17°, a shuttle pre-tilt of 45°, and a FIB beam tilt of 52° relative to the plummet, the lamella pre-tilt is 10°, which just about meets the preferred angular range of ±60° in the TEM by tilting from -50° to +70°, the maximum of many TEM cryo-holders.

3.5. Take an SEM image of the same square to help with the identification of corresponding beads in the fluorescence and ion beam view.

3.6. Perform registration of the deconvolved 3D FLM stack and the 2D ion beam view for each position with the 3DCT as described in the following (**Figure 4B**) steps.

3.6.1. Load the corresponding resliced 3D FLM stack and ion beam (IB) view in 3DCT.

NOTE: Multi-color fluorescence data can be loaded as up to three separate single-channel stack files.

3.6.2. Select 4 fiducial beads in the fluorescence data and right-click on the positions list to determine their 3D position *via* Gaussian fitting of the signal in x, y, and z. Select the corresponding beads in the IB image and perform an initial 3D correlation (correlate).

3.6.3. Iteratively add more beads in the fluorescence image, refine their 3D position, and predict their position in the IB view to quickly add more beads to the registration and to check the accuracy of the correlation. In 3DCT, root-mean-square error (RMSE) values are provided to assess the correlation consistency[7].

3.6.3.1. Ensure that the RMSE values are small and on the order of the localization accuracy (~300 nm). To determine the accuracy of the correlation, leave out some fiducial beads clearly identifiable in both fluorescence and ion beam deliberately during the registration step. Do this by checking their predicted versus actual location in the ion beam image. If the predicted position differs significantly from the real, repeat the initial correlation with a new set of fiducials.

NOTE: Correlating 6–8 beads has proven sufficient for accurate registration of the FLM stacks and the IB views. However, adding more fiducials (up to 12–15) over a wide range of z values (e.g., by selecting beads on the grid bar or in neighboring squares) may improve the accuracy of correlation.

3.6.4. Select the targeted cellular signals, fit their 3D position in the FLM stack and apply the transformation to predict the target positions in the IB view (**Figure 4B**).

NOTE: Any entry in the FLM positions list, which does not have a counterpart in the IB list, will be treated as a signal to be predicted.

3.7. For each correlated square, transfer predicted positions of the features of interest to the FIB-SEM instrument and place lamella milling patterns (**Figure 4C**). Transfer positions manually (e.g., by measuring the distance to visible landmarks, such as cells or fiducial beads) or use automation and scripting as implemented, for example, in SerialFIB[14]. If there are multiple signals per cell, place the patterns to include as many points-of-interest (POIs) as possible in the same lamella to increase throughput.

3.8. First rough, and then fine mill the lamellas to a final thickness of 150–250 nm. Avoid steps (e.g., stress relief cuts[15]) that cause sagging of the lamella and thus result in movement of the actual feature of interest with respect to the previously acquired FLM stacks. Use either manual[3] or automated[14,16–18] FIB milling procedures. With either method, ensure that the feature of interest remains in the center of the lamella by symmetrically thinning it from the top and bottom.

3.9. To evaluate the accuracy of milling for each lamella, perform the same registration as in step 3.4. However, this time, use the final IB image after FIB milling and check whether the predicted positions of the features of interest are contained within the final lamella. Alternatively, overlay the rotated projections of the FLM stacks, obtained from 3DCT's output and custom scripts[19], with the final IB image (**Figure 4C**, small insert).

[Place **Figure 4** here]

4. Correlative TEM

4.1. Load the grids into the TEM, making sure that lamella orientation (as apparent from cutout or orientation marks) is perpendicular to the tilt axis.

NOTE: Microscopes of different manufacturers can be controlled using various software, e.g., Tomo5, TOM, or SerialEM[20]. Here, the focus is on the latter.

4.2. Acquire grid montage and overviews for each grid square containing lamellas. Ensure that the magnification and exposure time is suitable to visualize the fiducial beads in the TEM images without significantly adding to the total electron dose. Acquire high-resolution TEM maps (montages) of each lamella.

4.3. Register and 3D-2D correlate the FLM stack with the TEM grid square and the lamella overviews in 3DCT. Use the same procedure as described in step 3.6 by selecting corresponding bead positions in the fluorescence (x, y, z - gaussian fit) and transmission electron microscope images. Then, select the positions of interest in the FLM channels and transfer them to the TEM overviews. If necessary, use a two-step procedure comprising a first correlation between FLM

and low magnification TEM, and second one from low to high magnification TEM (**Figure 5**).

4.4. Transfer positions either manually (by measuring distances to landmarks, the registration and map tools available within SerialEM[20]), or external software such as CorRelator[21].

4.5. Set up and run tilt-series at correlated positions. Use an appropriate magnification, defocus, and total dose (see **Table of Materials** and **Table 1** for details). Start the acquisition at the pre-tilt determined by the lamella (also see the note in step 3.4) and use a dose-symmetric tilt scheme[22]. Use either manual or batch acquisition.

[Place **Figure 5** here]

REPRESENTATIVE RESULTS:

The protocol provides a walk-through of the pipeline used to discover the EH domain-containing and endocytosis protein 1 (Ede1)-dependent endocytic protein deposit (END) and its degradation and trapping in autophagic bodies[8]. The END is a liquid-liquid phase-separated compartment in *S. cerevisiae*, which buffers a variety of proteins involved in clathrin-mediated endocytosis (CME) after failed endocytic events. One of its main components is Ede1, which doubles as a CME component and as a selective autophagy receptor for the degradation of this new LLPS compartment. Accordingly, an EGFP fusion of Ede1 (EGFP-Ede1) under the control of the alcohol dehydrogenase (ADH) promoter was used to visualize ENDs since Ede1 overexpression interferes with the early stages of endocytosis and therefore constitutively induces LLPS.

On a plunge-frozen grid with EGFP-Ede1 overexpressing yeast cells and 1 µm fiducial markers, five positions were selected for FLM stack acquisition in the GFP channel (**Figure 6A**; TFS Corrsight; confocal mode, 300 nm focus step size, 10 µm range). The grid was transferred to the FIB instrument (Quanta 3D FEG), and the grid squares for which FLM stacks had been acquired were identified by performing a 2D-2D correlation of the fluorescence and SEM grid overviews (compare step 3.2).

For each of the chosen squares, ion beam images were taken at a low current (10 pA, 1200x magnification), and corresponding fiducial positions were registered in 3DCT. After selection of positions with the biological feature of interest and fitting their 3D position within the FLM stack, the found transformation was applied to putative END positions, and the sites for lamella preparation were selected (**Figure 6B**). A FIB beam inclined 11° relative to the grid surface was used in the examples shown here (45° FIB shuttle pre-tilt; 18° stage tilt). Positions of interest were transferred, and FIB patterns were drawn manually (**Figure 6D**) by measuring the distance of the predicted positions relative to prominent landmarks in the FIB image (e.g., holes, ice contaminations, fiducial beads). The accuracy of the registration was evaluated by deliberately leaving out beads that could clearly be identified in the FLM and IB image, and then comparing their actual and predicted positions in the ion beam view (e.g., diamond in **Figure 6B**,**C**). The correlation for the square shown in **Figure 6C** was found to be accurate (i.e., the predicted position of FLM bead positions perfectly coincided with their corresponding IB location and 3DCT reported sub-pixel RMSE values for the registration). Thus, lamellas were cut at the predicted

positions (Site B) and fine-milled to a thickness of ~200 nm (final pattern offset).

[Place **Figure 6** here]

After successful FIB milling and transfer of the grid to the cryo-transmission electron microscope (Titan Krios operated at 300 kV and equipped with a Gatan K2 direct electron detector and Bioquantum energy filter), a grid overview was recorded in SerialEM and used to locate squares with lamellas. For each lamella, overview images were acquired, and the FLM data was registered in 3DCT (3D-2D) using corresponding fiducial beads. Positions of the biological features of interest (**Figure 7A**) were then predicted using the transformation calculated from the fiducial beads. Lamella overviews recorded at higher magnification were stitched, and sites of interest correlated using clearly visible landmarks (e.g., fiducial beads). Alternatively, classical CLEM overviews can be produced in various softwares[10,12].

Based on the correlation, four potential sites for tomogram acquisition were found for the lamella shown in **Figure 7A**. However, this also includes a position that was not targeted during the 3D-correlated FIB-milling (compare **Figure 6D**; gray circle) and a position blocked by ice contamination (**Figure 7**; gray boxes). Accordingly, tomograms could only be recorded for two positions (**Figure 7B**). Overall, a correlation success of ~75%, i.e., lamellas that survived the transfer to the TEM and END structures were found at the predicted sites, was achieved (12 correlated sites). After tomogram reconstruction, segmentation and template matching, individual END structures can be visualized within their native context (**Figure 7C,D**). This includes the fenestrated endoplasmic reticulum (ER) surrounding the END, lipid droplets occasionally making contact, and ribosomes, which are excluded from the LLPS compartment. Taken together, this shows how 3D-correlative FIB milling can provide molecular-level information of rare biological processes from intact cells.

[Place **Figure 7** here]

FIGURE AND TABLE LEGENDS:

Figure 1: Summary of the workflow with a selection of critical steps. The entire protocol is divided into four stages according to the equipment used: Sample preparation, including plunge freezing, cryo-fluorescence microscopy, cryo-focused ion beam milling, and cryo-electron microscopy. For each step, several key points are highlighted.

Figure 2: Screening for suitable grids using SEM and IB. (**A**) Orientation marks should be placed on the AutoGrids perpendicular to the milling direction to simplify correct loading into the TEM. Cells are mounted facing up in the assembled AutoGrid. (**B**) After plunge freezing, grids are inspected in the SEM to evaluate and optimize plunging conditions: a) There should not be too many cells per grid. For HeLa cells, for example, do not use more than 1–4 cells/square. For smaller cells such as *Saccharomyces cerevisiae* (shown here), clumps of 4–6 cells have been found useful. b) Fiducial beads (white arrows) should clearly be visible, and there should not be too much buffer surrounding the cells.

Figure 3: Selecting squares for FLM stack acquisition and improvement of data by deconvolution. (**A**) Overview of a grid plunged with yeast cells expressing eGFP-Ede1 (green) and mCherry-Atg8 (magenta). Choose positions with a good distribution of beads and cells, but avoid the edges of the grid (shaded red). The boxes indicate positions with good cell distributions where fluorescence stacks were taken. (**B**) Maximum intensity projection (MIP) of the multi-color stack taken on the yellow-boxed square (from A) after deconvolution. Deconvolution of the FLM stacks significantly cleans up unwanted background signals and helps localize beads in z more accurately, as apparent from gaussian fits before (**C**) and after deconvolution (**D**) (fits were performed in 3DCT and are shown for the bead marked with 1). Images show zoomed-in MIP views of the red channel (excitation: 552 nm, emission: 585–650 nm).

Figure 4: 3D-correlative FIB milling procedure. (**A**) 2D-2D correlation of FLM (left) and SEM (right) overviews of the grid is used to locate the grid squares on which fluorescent stacks were taken previously. (**B**) For each selected square, after 3D-2D registration of corresponding fiducial positions in 3DCT (colored boxes), positions of biological features of interest are selected in the FLM data. Based on the prediction of corresponding positions in the ion beam image (red circles), sites for lamella preparation are selected. (**C**) Scanning electron microscope (SEM) and ion beam (IB) images are used to keep the target centered during milling. Final thicknesses of 150–250 nm have been found adequate for further downstream processing.

Figure 5: Localization of correlated positions in the TEM. After successful 3D-correlative FIB milling and transfer to the transmission electron microscope, 3D-2D registration is performed for each milled square between fiducial beads (colored boxes) in FLM stacks and TEM overviews to localize potential sites for cryo-ET (red circles). Higher magnification lamella overviews (zoom-in) can then be acquired to set up tomograms more precisely.

Figure 6: Representative results for 3D-correlative targeting of endocytic protein deposits (END) in yeast. (**A**) SEM overview of the grid before milling. The colored boxes indicate grid squares for which fluorescence stacks were taken beforehand. (**B–C**) 3D correlation in a grid square. After registering several corresponding fiducial beads (colored boxes) in the FLM data (**B**, shown here as maximum intensity projection) and the ion beam image (**C**), the accuracy of the 3D registration was verified by predicting the position of the bead indicated with the diamond. Next, the positions of the target signal (red circles) were predicted in the ion beam view for two potential milling sites. (**D**) Zoom-in of Site B showing the predicted positions of three target puncta (red circles) and the initial milling patterns (yellow boxes). A fourth fluorescence punctum was predicted to be much lower than the other puncta and therefore not targeted during milling (gray circle).

Figure 7: Representative results for visualizing the END with cryo-ET. (**A**) The low magnification TEM overview of the milling site shown in **Figure 6** can readily be correlated with the FLM maximum intensity projection (**Figure 6B**) to localize biological features of interest (red crosses). (**B**) In a second step, a higher magnification (stitched) view can be correlated, and positions for tomogram acquisition (yellow boxes) are set up. Locations resulting from the out-of-plane signal (gray box, compare **Figure 6D**) were ignored. (**C–D**) Using this 3D-correlative FIB approach, the

endocytic protein deposit (END) can be visualized in its native environment. Structures such as the endoplasmic reticulum (ER), ribosomes, membranes, and lipid droplets can be identified and visualized.

Table 1: List of tested equipment and suggested settings.

DISCUSSION:

Optimization of cell culture and grid plunging parameters is fundamental for this workflow. At the beginning of a project, it is worth investing time to optimize tagging strategies, the distribution of cells and fiducial beads, and test different grid preparation and blotting parameters. Working with an optimally plunge-frozen sample will significantly facilitate downstream processing.

As for any TEM experiment, vitreous samples are required. For large mammalian cells such as HeLa, 1–2 cells per grid square are preferable, but cells may still be vitreous at higher density. Optionally, vitrification can be improved in mammalian cells (e.g., HEK293, HeLa) by incubating them with 10% (v/v) glycerol added to the culture medium 10 min before plunging[23]. If available, grid patterning may be used to ensure perfect placement and distribution of the cells, thereby improving vitrification and later correlation[24].

While specific cells can be selected during the workflow, too few cells that show the biological feature of interest will significantly reduce overall throughput. To improve correlation in POI-positive cells, sufficiently bright fluorophores should be used. This is especially important at endogenous expression levels. We found that under cryo-conditions, mVenus often performed better than EGFP due to its increased brightness[25] and the hypsochromic shift, which keeps it suitable for standard GFP filter setups under cryo-conditions[26]. For non-point-like target structures, the trade-off between wavelength and localization accuracy (Abbe diffraction limit) should also be considered.

Efficient 3D-correlation also requires that grids are mechanically stable and are handled with great care. While standard gold or copper grids with carbon support may be used, the success rate may significantly be increased by using more rigid SiO_2 films depending on the project. However, it has not yet been conclusively determined whether (a) mechanical stability or (b) matching thermal expansion coefficients (substrate vs. film) to reduce cryo-wrinkling[27], is the most crucial factor for successful 3D correlation. Moreover, for picking up fragile Au grids, polydimethylsiloxane-coated dishes may be used[5].

In addition to ensuring sample stability, a careful choice of FLM imaging parameters is necessary for obtaining high-quality fluorescence stacks that are suitable for optimal targeting during FIB milling. In this regard, testing different denoising[28] or deconvolution techniques on the FLM data is also advised, as it may considerably improve the localization of fiducials and cellular signals. When correlating the fluorescence signal to FIB-SEM images, a good sampling of fiducial beads is important. They should be well distributed around the cells and possibly at different z heights. It is also good practice to validate the consistency of the correlation by checking the predicted vs.

actual positions of beads that were deliberately left out of the fiducial model but can clearly be correlated by eye. 3DCT's RMSE values should also always be considered to check the registration consistency.

Since the deposition of milled material and residual water from the FIB-SEM chamber (i.e., recontamination) increases the effective lamella thickness by adding amorphous material to both sides of it, keeping fine-milled lamellas in the microscope for a prolonged time generally reduces TEM data quality due to additional electron scattering events. Accordingly, milling is most often performed in a two-step fashion: first, all positions are milled roughly (i.e., to about 800 nm), and then finely (to ~150–250 nm), and the grid is immediately unloaded after the last lamella has been completed. Better correlation success may, however, be achieved by processing the positions of interest in a site-wise manner, hence performing rough and fine milling on the same lamella directly after one another since this leaves no time for bending or deformation. This, however, reduces the maximum number of lamellas that can be produced per grid depending on the recontamination rate of the system. For a rate of 20 nm/h, 4–6 lamellas are produced within 1–1.5 h.

Movement of the entire grid or the rough-milled lamellas >300 nm will result in poor or unsuccessful correlation (see also limitations discussed below). It should therefore be checked regularly, e.g., by comparing IB images before, during, and after FIB milling. Sites that show significant movement (>300 nm) should be discarded. Optimize the sample preparation (i.e., choice of grid type, cell density, and plunging parameters; see protocol section 1) and milling strategy to avoid these movements. Lamella bending can significantly be reduced by site-wise milling as described in step 3.6 and reducing the lamella width. As mentioned before, while stress relief cuts[15] have been designed to reduce lamella bending, they often result in a concerted movement of the de-coupled lamella, thereby effectively preventing correlation. Integrated FLM systems may be used to solve this problem.

It is highly advised to perform a thorough characterization of the sample in live-cell imaging before going to cryo-conditions. Optimizing the cellular samples, treatment schemes, and knowing what kind of signal to expect before entering the cryo-workflow can substantially improve its success rate.

In the workflow presented here, a stand-alone fluorescence microscope with a cryo-stage is used to image the samples, followed by a transfer of the grids into the focused ion beam microscope. However, it has been tested on systems where a fluorescence microscope is integrated into the FIB-SEM chamber, and therefore no sample transfer is required to acquire fluorescence images[29–31]. Using such integrated systems, positions of interest can be imaged during and after FIB milling to check for the presence of the target fluorescence signal without increasing the risk of contaminating the final lamellas. It is, however, important to keep in mind the optical parameters of the used microscopes, as, e.g., a low NA objective will limit the precision with which fiducial beads and target signals can be localized. Nonetheless, integrated FLM setups will help to also better deal with slight deformations of grids and lamellas, as FLM stacks can continuously be updated and compared to up-to-date SEM and IB views.

As an alternative to fluorescence imaging of the lamella between FIB milling and TEM data acquisition, post-TEM correlation can be used to verify correct placement and milling of the lamellas[5,6].

During all steps of the correlative workflow, but especially during TEM, it is recommended to create an overlay of the projected fluorescence data on the FIB-SEM/TEM images. Such classical CLEM views help understand more intuitively which part of the cells is contained within the lamellas. This also serves as a useful sanity check to verify the accuracy of the correlation.

The 3D-correlative FIB approach requires samples that can be supplied with fiducial beads. Accordingly, this method is presently restricted to plunge-frozen grids. For high-pressure (HPF) frozen (tissue) samples, presently, only 2D-2D correlations can be performed. Potentially, internal fiducial markers (e.g., organelles, stained lipid droplets) could be a solution to this problem[32,33]. The final correlation success rate depends on many factors, including the sample quality, the fluorescence microscopy setup, the lamella thickness, and the size of the targeted structure. The correlation accuracy using the described 3D registration approach is estimated to be in the range of 200–300 nm on the final IB image, roughly corresponding to the typical thickness of FIB-milled lamellas[7]. Accordingly, cellular structures much smaller than this will be hard to target at present. Additionally, excessive movement at the milling site (>300 nm) also reduces the accuracy of the correlation, an issue that can potentially be addressed with FLM setups integrated into FIB/SEM instruments. Lamellas that show strong deformation or bending during milling should, in any case, be excluded from the downstream workflow.

Overall, cryo-fluorescence imaging is currently limited by the Abbe diffraction criterion. With more routine application (and commercialization) of super-resolved cryo-FLM methods, more accurate targeting of cellular structures might become possible, especially when integrated into the FIB/SEM for on-the-fly operation.

Especially in comparison to non-targeted and post-correlation techniques, the 3D-correlated FIB milling approach allows the selection of suitable positions before the time- and resource-consuming TEM step. It, thereby, enables more efficient data collection and project planning. Moreover, the correlated fluorescence data adds a layer of information that can be crucial for interpreting the tomograms and for integrating the cryo-ET results in multi-scale projects, especially when dealing with non-structured protein assemblies or those too small for template matching and subtomogram averaging.

In combination with advanced workflows such as cryo-lift out of HPF samples[34,35], cryo-FIB-SEM volume[36] and super-resolution fluorescence imaging[26,37–39], 3D-targeted lamella preparation offers the prospect of not only dissecting biological processes in isolated cells but also to make tissue and patient samples accessible to FIB milling and cryo-electron tomography. As such, it will allow dissection of pathological processes at high resolution and thus be an integral building block toward a biopsy at the nanoscale.

ACKNOWLEDGMENTS:

We thank Inga Wolf for supporting the IT infrastructure, Florian Beck for computational support, and Oda H. Schiøtz for the critical reading of the manuscript. Funding was provided in part through an Alexander von Humboldt returners fellowship to Philipp S. Erdmann and an EMBO Long-term Fellowship ALTF 764-2014 to Florian Wilfling. Anna Bieber was supported by a Boehringer Ingelheim Fonds Ph.D. fellowship.

DISCLOSURES:

The authors declare no conflicts of interest.

REFERENCES:

1. Beck, M., Baumeister, W. Cryo-Electron tomography: Can it reveal the molecular sociology of cells in atomic detail? *Trends in Cell Biology*. **26** (11), 825–837 (2016).
2. Plitzko, M., Villa, E., Schaffer, M., Baumeister, W. Opening windows into the cell : focused-ion-beam milling for cryo-electron tomography. *Current Opinion in Structural Biology*. **23**, 771–777 (2013).
3. Schaffer, M. et al. Optimized cryo-focused ion beam sample preparation aimed at in situ structural studies of membrane proteins. *Journal of Structural Biology*. **197** (2), 73–82 (2017).
4. Tegunov, D., Xue, L., Dienemann, C., Cramer, P., Mahamid, J. Multi-particle cryo-EM refinement with M visualizes ribosome-antibiotic complex at 3.5 Å in cells. *Nature Methods*. **18** (2), 186–193 (2021).
5. Klein, S., Wachsmuth-Melm, M., Winter, S. L., Kolovou, A., Chlanda, P. *Cryo-correlative light and electron microscopy workflow for cryo-focused ion beam milled adherent cells. Methods in Cell Biology*. Elsevier Inc. **162**, 273-302 (2021).
6. Klein, S. et al. Post-correlation on-lamella cryo-CLEM reveals the membrane architecture of lamellar bodies. *Communications Biology*. **4** (1), 1–12 (2021).
7. Arnold, J. et al. Site-Specific Cryo-focused ion beam sample preparation guided by 3D correlative microscopy. *Biophysical Journal*. **110** (4), 860–869 (2016).
8. Wilfling, F. et al. A selective autophagy pathway for phase-separated endocytic protein deposits. *Molecular Cell*. **80** (5), 764–778.e7 (2020).
9. Scientific volume imaging, Nyquist calculator at <https://svi.nl/NyquistCalculator> (2021).
10. Schindelin, J. et al. Fiji: an open-source platform for biological-image analysis. *Nature Methods*. **9** (7), 676–682 (2012).
11. Huygens Professional version 19.04 (Scientific Volume Imaging, The Netherlands) at < http://svi.nl> (2021).
12. de Chaumont, F. et al. Icy: an open bioimage informatics platform for extended reproducible research. *Nature Methods*. **9** (7), 690–696 (2012).
13. Arnold, J. 3DCT at <https://3dct.semper.space/> (2021).
14. Klumpe, S. et al. A modular platform for streamlining automated cryo-FIB workflows. *bioRxiv*. 2021.05.19.444745 (2021).
15. Wolff, G. et al. Mind the gap: Micro-expansion joints drastically decrease the bending of FIB-milled cryo-lamellae. *Journal of Structural Biology*. **208** (3), 0–3 (2019).
16. Buckley, G. et al. Automated cryo-lamella preparation for high-throughput in-situ structural biology. *Journal of Structural Biology*. **210** (2), 107488 (2020).

17. Tacke, S. et al. A streamlined workflow for automated cryo focused ion beam milling. *bioRxiv*. 2020.02.24.963033 (2020).
18. Zachs, T. et al. Fully automated, sequential focused ion beam milling for cryo-electron tomography. *eLife*. **9**, e52286 (2020).
19. Fung, H. K. H. tools3dct at <https://github.com/hermankhfung/tools3dct> (2021).
20. Mastronarde, D. N. Automated electron microscope tomography using robust prediction of specimen movements. *Journal of Structural Biology*. **152** (1), 36–51 (2005).
21. Yang, J. E., Larson, M. R., Sibert, B. S., Shrum, S., Wright, E. R. CorRelator: Interactive software for real-time high precision cryo-correlative light and electron microscopy. *Journal of Structural Biology*. **213** (2), 107709 (2021).
22. Hagen, W. J. H., Wan, W., Briggs, J. A. G. Implementation of a cryo-electron tomography tilt-scheme optimized for high resolution subtomogram averaging. *Journal of Structural Biology*. **197** (2), 191–198 (2017).
23. Bäuerlein, F. J. B. et al. In situ architecture and cellular interactions of polyQ inclusions. *Cell*. **171** (1), 179–187 (2017).
24. Toro-Nahuelpan, M. et al. Tailoring cryo-electron microscopy grids by photo-micropatterning for in-cell structural studies. *Nature Methods*. **17** (1), 50–54 (2020).
25. Shaner, N. C., Steinbach, P. A., Tsien, R. Y. A guide to choosing fluorescent proteins. *Nature Methods*. **2** (12), 905–909 (2005).
26. Kaufmann, R. et al. Super-resolution microscopy using standard fluorescent proteins in intact cells under cryo-conditions. *Nano Letters*. **14** (7), 4171–4175 (2014).
27. Booy, F. P., Pawley, J. B. Cryo-crinkling: what happens to carbon films on copper grids at low temperature. *Ultramicroscopy*. **48** (3), 273–280 (1993).
28. Krull, A., Buchholz, T. O., Jug, F. Noise2void-Learning denoising from single noisy images. *Proceedings of the IEEE Computer Society Conference on Computer Vision and Pattern Recognition*. **2019**-**June**, 2124–2132 (2019).
29. Gorelick, S. et al. PIE-scope, integrated cryo-correlative light and FIB/SEM microscopy. *eLife*. **8**, 1–15 (2019).
30. Delmic METEOR at <https://www.delmic.com/en/products/cryo-solutions/meteor> (2021).
31. Scientific, T. F. iFLM at <https://assets.thermofisher.com/TFS-Assets/MSD/Datasheets/iflm-aquilos-datasheet-ds0366.pdf> (2021).
32. Mahamid, J. et al. Liquid-crystalline phase transitions in lipid droplets are related to cellular states and specific organelle association. *Proceedings of the National Academy of Sciences of the United States of America*. **116** (34), 16866–16871 (2019).
33. Scher, N., Rechav, K., Paul-Gilloteaux, P., Avinoam, O. In situ fiducial markers for 3D correlative cryo-fluorescence and FIB-SEM imaging. *iScience*. **24** (7), 102714 (2021).
34. Mahamid, J. et al. A focused ion beam milling and lift-out approach for site-specific preparation of frozen-hydrated lamellas from multicellular organisms. *Journal of Structural Biology*. **192**, 262–269 (2015).
35. Schaffer, M. et al. A cryo-FIB lift-out technique enables molecular-resolution cryo-ET within native Caenorhabditis elegans tissue. *Nature Methods*. **16** (8), 757–762 (2019).
36. Wu, G.-H. et al. Multi-scale 3D cryo-correlative microscopy for vitrified cells. *Structure*. **28** (11), 1231–1237.e3 (2020).

37. Liu, B. et al. Three-dimensional super-resolution protein localization correlated with vitrified cellular context. *Scientific Reports*. **5** (October), 13017 (2015).
38. Weisenburger, S., Jing, B., Renn, A., Sandoghdar, V. Cryogenic localization of single molecules with angstrom precision. *SPIE NanoScience + Engineering*. **8815**, 88150D (2013).
39. Tuijtel, M. W., Koster, A. J., Jakobs, S., Faas, F. G. A., Sharp, T. H. Correlative cryo super-resolution light and electron microscopy on mammalian cells using fluorescent proteins. *Scientific Reports*. **9** (1), 1–11 (2019).

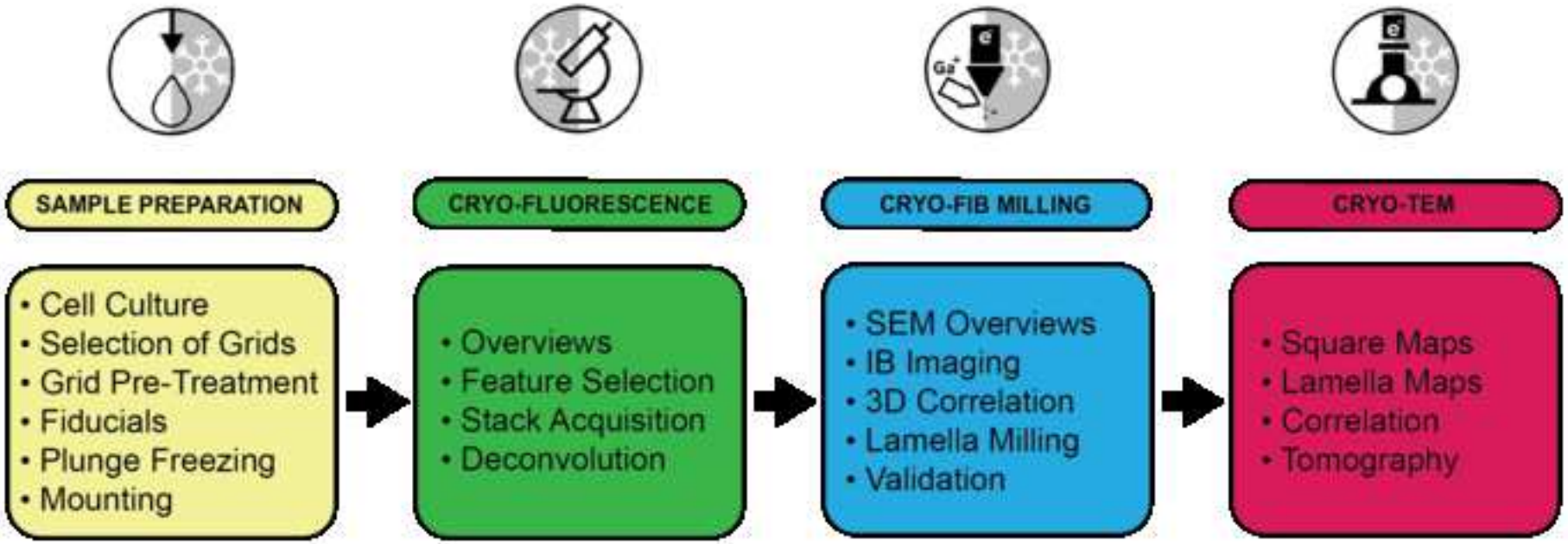

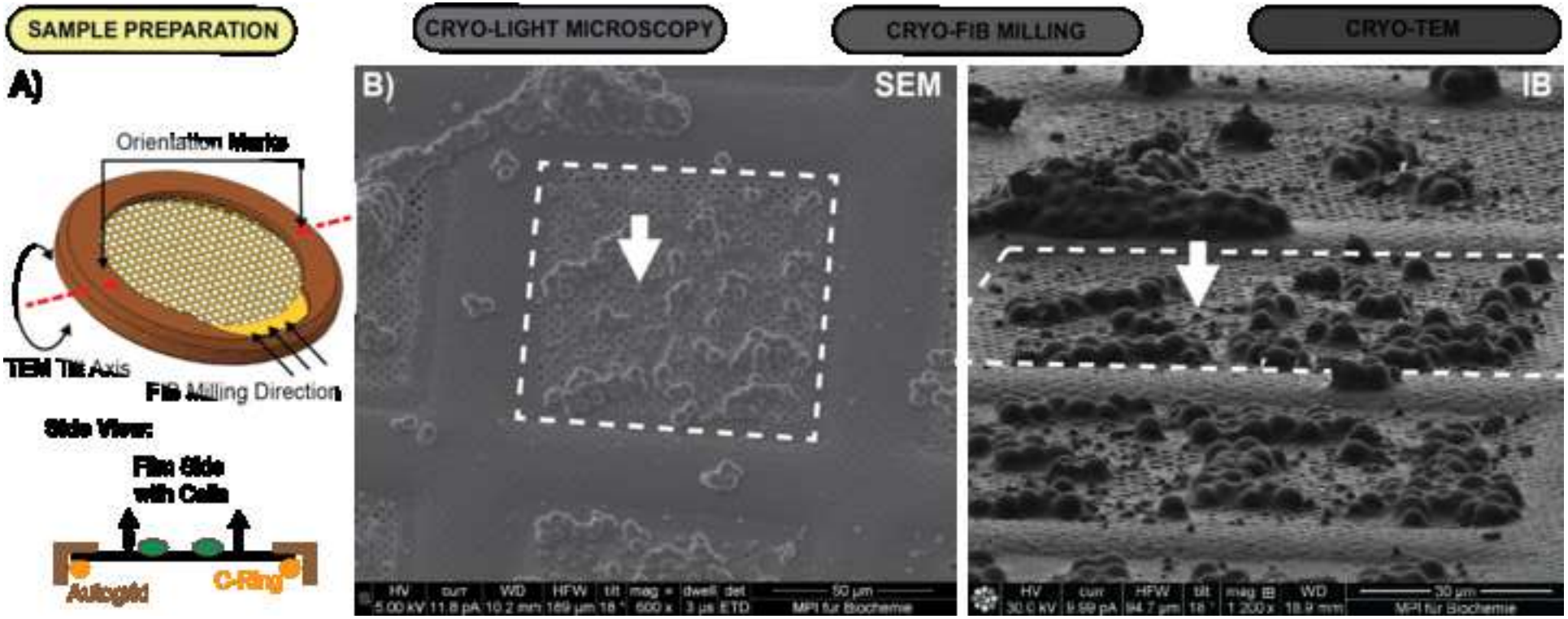

Revised Figure 3

Click here to access/download;Figure;3DC-FIB_JOVE_PSErdmann_Figure_3.png

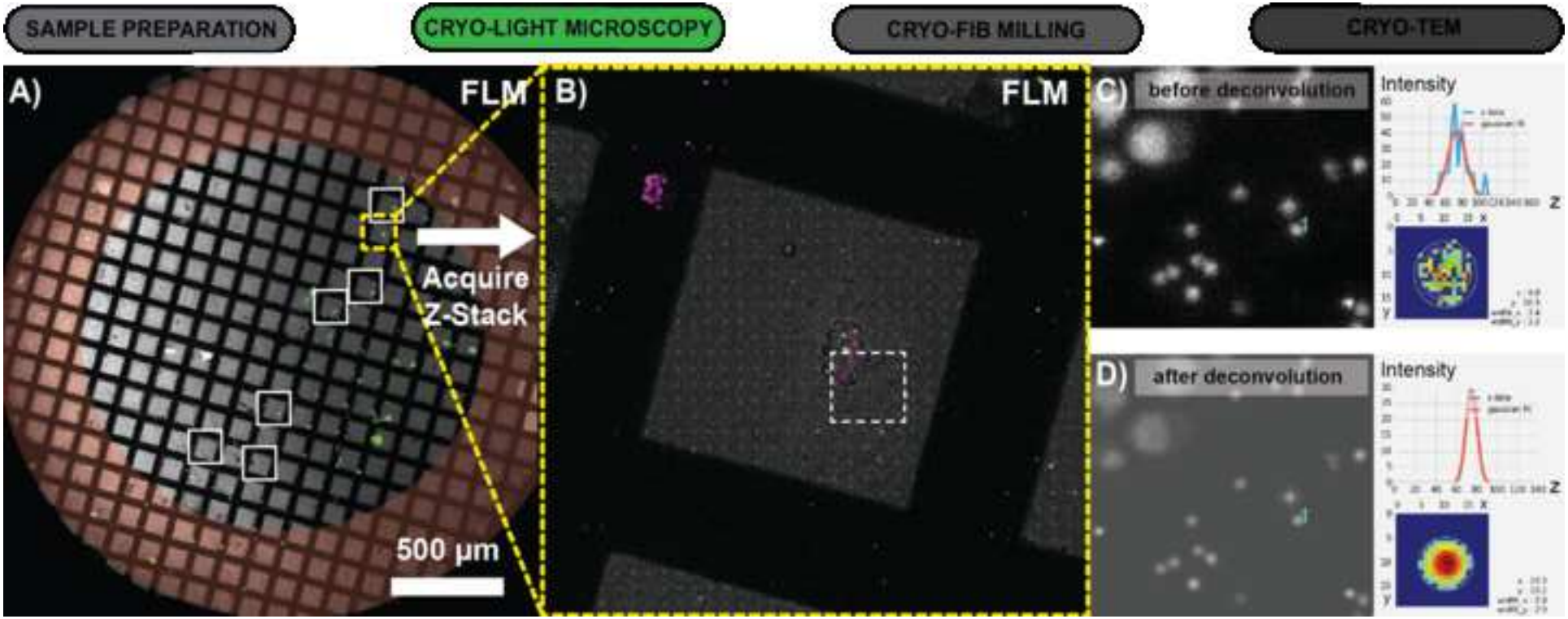

Revised Figure 4

Click here to access/download;Figure;3DC-FIB_JOVE_PSErdmann_Figure_4.png

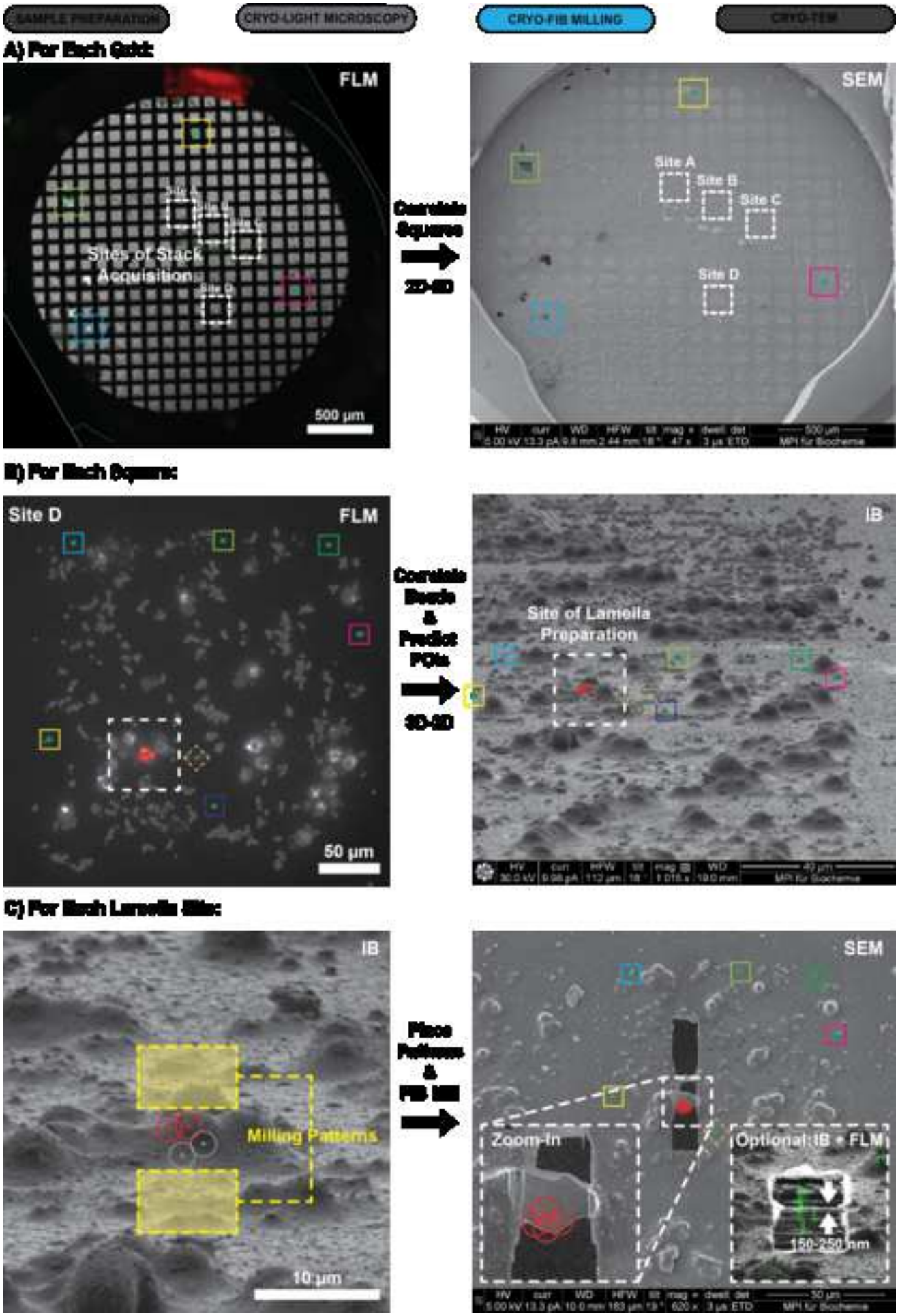

Revised Figure 5

Click here to access/download;Figure;3DC-FIB_JOVE_PSErdmann_Figure_5.png

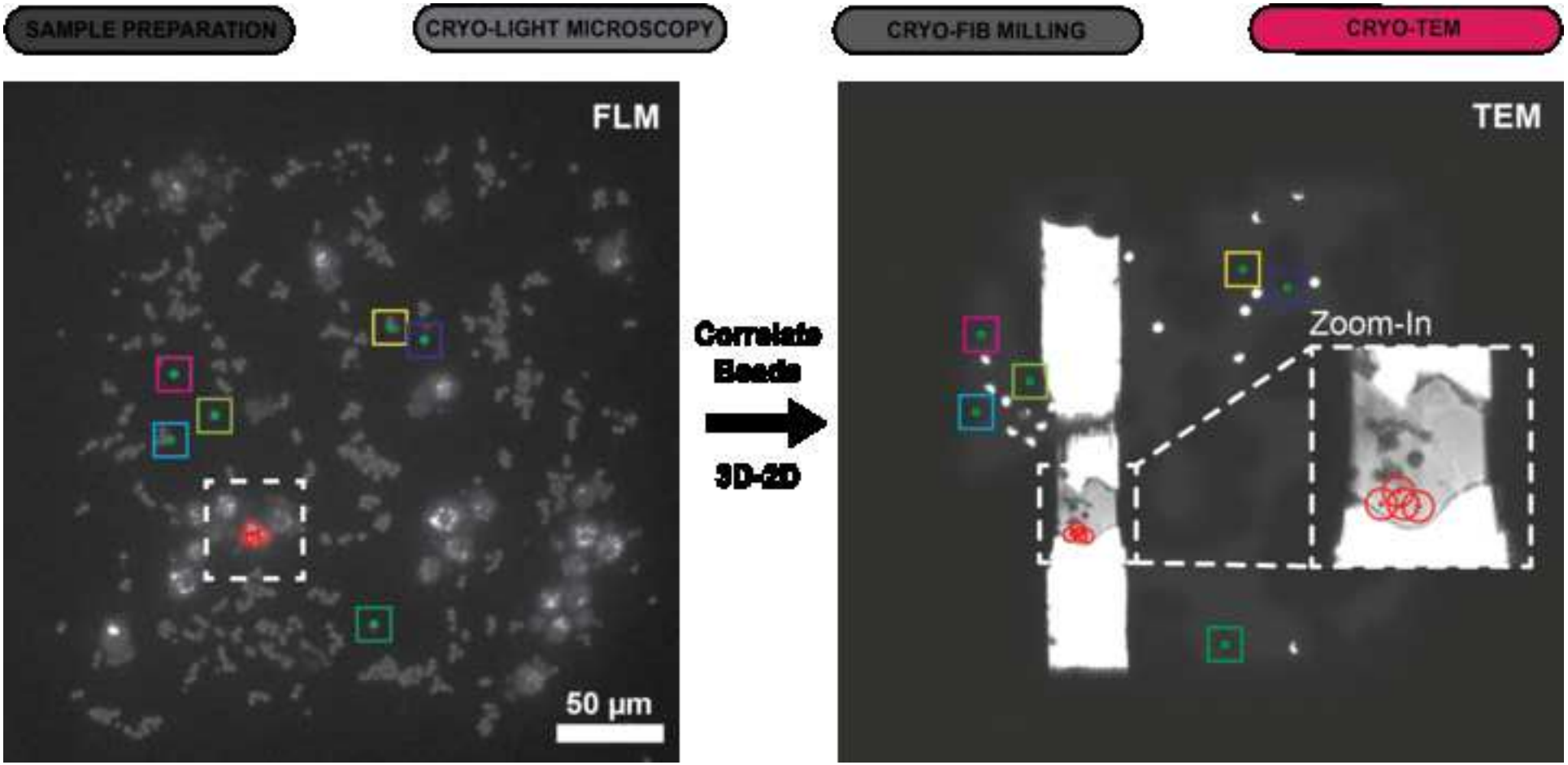

Revised Figure 6

Click here to access/download;Figure;3DC-FIB_JOVE_PSErdmann_Figure_6.png

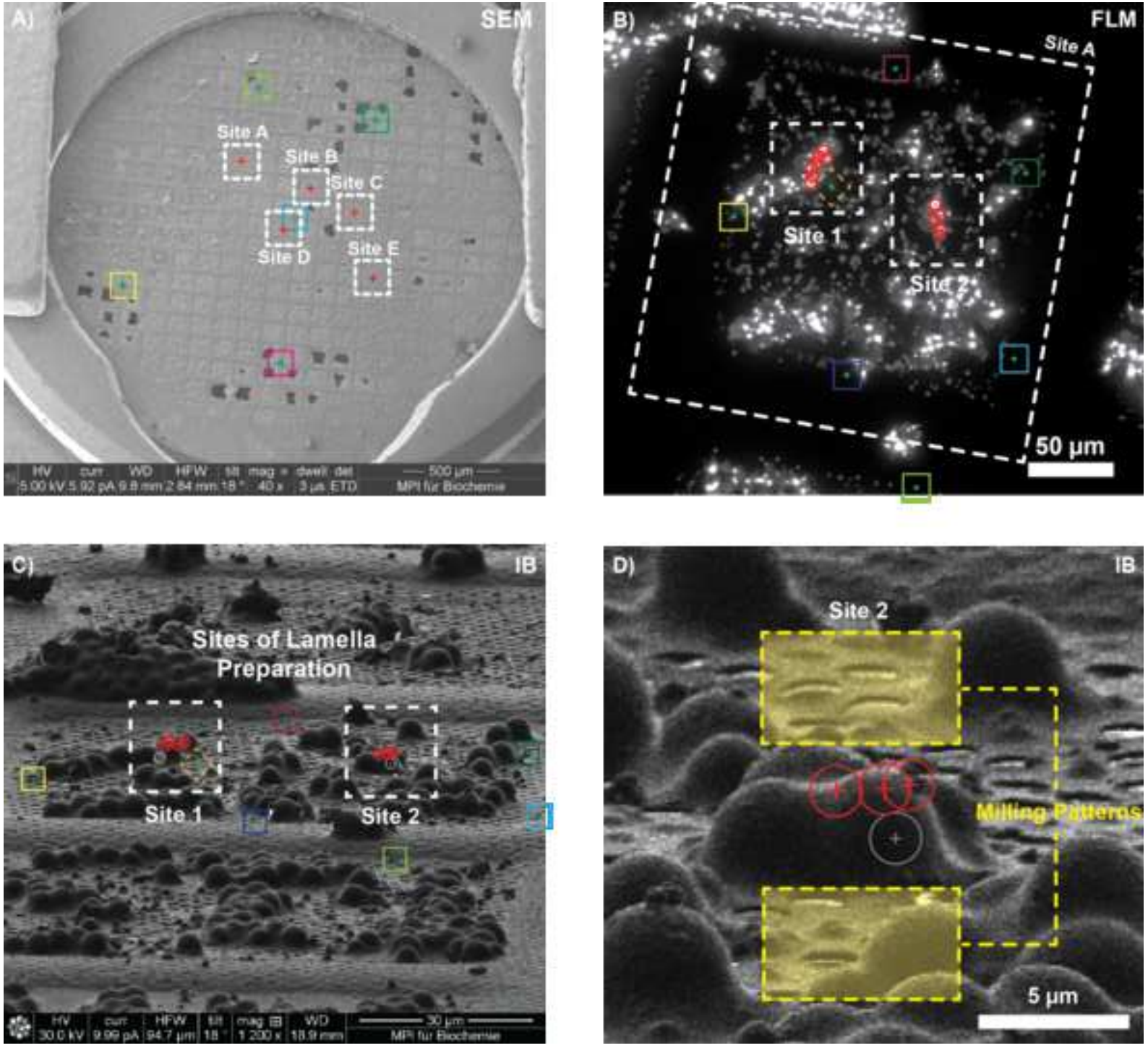

Revised Figure 7

Click here to access/download;Figure;3DC-FIB_JOVE_PSErdmann_Figure_7.png

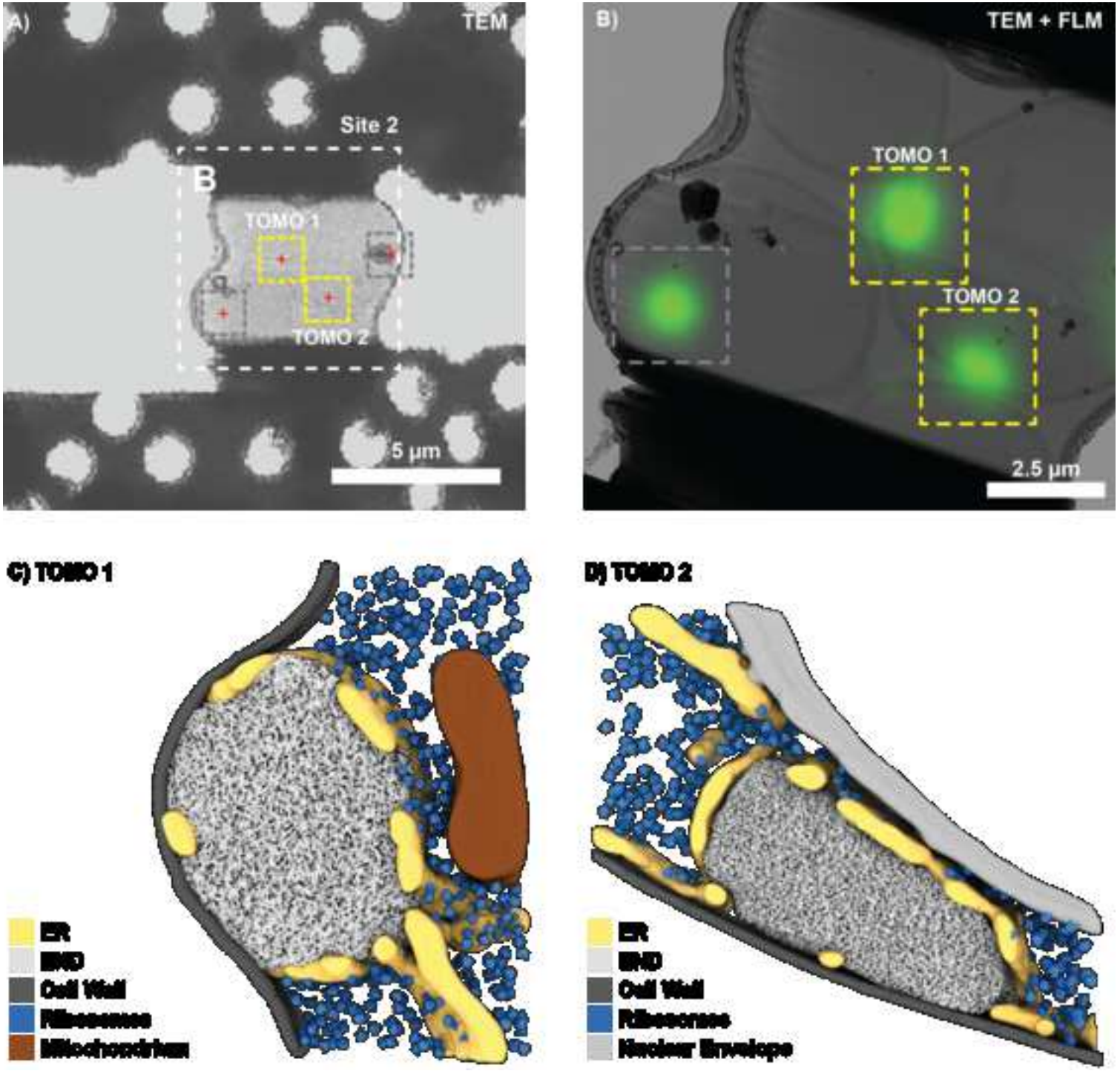

Plasma Cleaner Settings
Harrick Plasma Cleaner PDG-3XG :

Plunger Settings
TFS Vitrobot Mk IV:

FIB GIS Positions and Timings
Quanta 3D FEG:
TFS Scios:
TFS Aquilos 1:
TFS Aquilos 2:

FIB Sputter Coater Settings
Quorum System:
TFS Scios:
TFS Aquilos 1:
TFS Aquilos 2:

Tomogram Acquisition
Titan Krios Gi2

Titan Krios Gi4

FLM Acquisition
Corrsight (Confocal Mode)
Leica SP8 Cryo-Confocal

Radio Frequency setiing: "HI", 30 s; N2 plasma

100% humidity; blotforce = 8; blottime = 10 s; wait time 0 s; (this should work for most suspension and adherent cells)

Tilt = 0, Rotation = -180, Z position = 13.5, Temperature setpoint =26.15° , Time = 8 s
Tilt = 0, Rotation = -180, Z position = 9.8, Temperature setpoint =28° C, Time = 7 s
Software predefined position, Temperature setpoint = 28° , Time = 7 s
Software predefined position, Temperature setpoint = 28°, Time = 7 s

In Quorum prep chamber: 10 mA, 40 s
10 W, 500 V, 250 mA, 0.2 mbar, 15 s
1kV, 10 mA, 10 Pa, 15 s
1kV, 10 mA, 10 Pa, 15 s

K2 camera, Gatan Bioquantum energy filter
20 eV slit; dose symmetric tilt scheme (Hagen) with 2° steps; start at +10° (lamella pre-tilt!) to +70°and -50°
Falcon 4; Selectris X energy filter
10 eV slit; dose symmetric tilt scheme (Hagen) with 2° steps; start at +10° (lamella pre-tilt!) to +70° and -50°

Objective: Zeiss EC Plan-Neofluar 40×/0.9 NA Pol; Stack acquisition parameters: x-y pixel size = 161.25 nm, z step size =
Objective: Leica HCX PL APO 50x / 0.90 CLEM; Stack acquisition parameters: x-y pixel size = 84 nm, z step size = 300 nm

= 300 nm.

ɲ.

Dr. Philipp S. Erdmann
Group Leader
Fondazione Human Technopole
philipp.erdmann@fht.org

21/07/21

To: The Editor
Journal of Visualized Experiments (JOVE)

Submission of a Revised Manuscript

Please find attached our revised manuscript entitled “Sample Preparation by 3D-Correlative Focused Ion Beam Milling for High-Resolution Cryo-Electron Tomography” and our point to point response to the reviewers’ comments. We would like to thank both reviewers and the editor for the constructive feedback and hope that our protocol is now suitable for filming and publication in JOVE.

Sincerely yours,

Philipp S. Erdmann
Research Group Leader in Structural Biology
Fondazione Human Technopole

Reviewers' comments:

Reviewer #1:

Manuscript Summary:

In the manuscript entitled ‚Sample Preparation by 3D-Correlative Focused Ion Beam Milling for High-Resolution cryo-Electron Tomography', Bieber et al. provide a protocol for correlative light and electron microscopy of focused ion beam milled cells after plunge freezing. This protocol is based on the pioneering work by Arnold et al. (2016) and was recently applied by Wilfling et al. (2020). Such a protocol is very welcomed and it will facilitate the application of this complex but important cryo-CLEM workflow in other labs of the cryo-EM community. However, as it is written now, the protocol lacks many important details.

Concerns:

The authors present the workflow in a generalized way, although it is very likely that the workflow was performed using Aquilos dual-beam microscope (Thermo Fisher Scientific) and a cryo-confocal microscope (Leica). This generalization leads to a lack of necessary details that are required to reproduce the presented workflow. It would be more valuable for the reader if the protocol would include details concerning the systems that were used.

Since there's only a "limited" selection of equipment available at our institute, these experiments were of course not performed and tested on all the FIB/SEMs and cryo-FLM setups that exist. We've added a statement commenting on this in the introduction. Nonetheless, we have sampled quite a significant space from Quanta 3D FEG to Scios, and Aquilos1/2 on the FIB/SEM side, and Corrsight, Leica Thunder, and Leica SP8 cryo as cryo-FLMs, which here serve as a basis for our generalized workflow. Individual settings for these instruments are now provided (see updated Materials xsl). However, the workflow doesn't change for any of these systems and hence we prefer to keeping the general tone. This might also help reduce the impression, that only the latest high-end equipment can be used for this workflow. In fact, the "Representative Results" we chose to show were prepared using the oldest machines in our list: Quanta3D FEG and Corrsight.

In addition, the authors should add a section on the compatibility of this protocol with different systems such as Zeiss cross-beams, Linkam cryo-LM, integrated cryo-LM-FIB-SEM, etc.

Unfortunately, places with access to FIB/SEM instruments other than the TFS brand are rare - even more so are the TEM alternatives and we haven't been able to test the

workflow there. However, we hope that the provided settings will allow experienced users to successfully transfer our workflow to other microscopes.

A discussion on integrated FLM solutions is present in the discussion section. However, most of these systems (iFLM, METEOR, PIE-Scope) have either not been delivered (yet), or are at a late prototype stage. Accordingly, significant changes (hardware/software) are to be expected. Due to this, we haven't added a detailed protocol on their use, yet. That said, we've tested and validated the approach on a prototype of Delmic's METEOR with great success.

In the following you can find a list of specific points which need to be addressed:
1) Line 42: "While it is possible to combine FLM and cryo-ET data only after TEM acquisition" Please also provide the reference of the detailed description of the mentioned method: doi.org/10.1016/bs.mcb.2020.12.009

In addition to the original publication, we now also direct the reader to the protocol.

2) Line 71: "Note: The structure of interest should be present in the majority of your cells, which will significantly increase the throughput of the correlative approach." This contradicts the statement in the abstract: Line 27-29: "Using this technique, rare cellular events and structures can be targeted with high accuracy and visualized at molecular resolution using cryo-transmission electron microscopy (cryo-TEM)".

We now explain this in more detail: while 3D-targeted FIB milling is in principle so selective that a single POI-positive cell/grid could be targeted, this would not be very productive as each time after finishing one lamella grids would have to be unloaded and a new sample placed in the FIB/SEM.

Since there is no publication showing that rare cellular events and structures can be targeted with high accuracy on lamella yet, the statement in the abstract should be revised.

Both Arnold et al. and Wilffiling et al. in fact show localization, targeting, and milling of structures ~ 500 nm in dimension on lamellas. In Wilfling et al., we used the approach on two different target structures: END compartments and autophagic bodies. For the END, 1-2 structures are present per cell (~rare). It is true of course that there is (among other limitations) a size limit. A detailed discussion on the limitations (and how they are related) is now present in the discussion section.

As the authors point out later in the manuscript the major limitations of the correlation are the Z resolution and the diffraction-limited resolution of FLM (Lines 399-401). One should point out that with the current setup a rare event can be targeted but it has to be a fairly large structure.

This is pointed out in the discussion section.

3) Line 76: "We significantly increased our success rate using more rigid SiO2 films." Please provide data that would prove the significance. In our experience, we have not found much of a difference between carbon and SiO2 but we do not have data to show it. It would be very useftul to the community if this was systematically tested and shown.

We agree that a systematic test would be preferable, but this would be outside the scope of this protocol. Our statement is more “qualitative”, summarizing the general experience in our department (several publications pending). Also, we want to point out alternatives for Au/C and Cu/C grids to (frustrated) FIB 3D correlation newcomers. Our suggestion is also in line with what has been reported for SPA (stability) and recently by Mahamid et al. in their SerialFIB pre-print, which suggest Ti/SiO_2 to be even better. Of course, the verdict is still out whether mechanical stability or matched thermal expansion coefficients (or both) is the determining factor for successful 3D FIB correlation. We’ve added an appropriate “disclaimer” to our statement.

4) Line 85: Which type of grids do you recommend for yeast, bacteria, adherent cells?

We’ve added a list of recommended grids.

5) Line 94: Note. Please provide the exact protocol on poly-L-lysin/concanavalin coating.

We’ve added the respective protocols.

6) Line 106: 4 Hela cells per square (200 Mesh) are too many as they would occupy the entire square and likely be poorly vitrified. 1-2 adherent cells are more desirable.

The text has been changed as suggested. While it is true that 1 cell/square would be ideal, depending on where lamellas are cut, we have observed vitreous HeLa calls at up to 4/5 cells/grid. We now also point out the potential use of glycerol as protective agent.

7) Line 107: Please provide more details on grid patterning and add a reference.

We've added a short explanation why grid pattering is useful and now provide the (missing) reference. For a detailed protocol, please refer to said publications as it is outside the scope of this protocol and also not required for successful 3D-correlative FIB milling.

8) Line 109: Please provide more details on how to remove grids carefully from the dish. This step is challenging and bent grids will negatively influence the outcome. 3D printed holders or the addition of the PDMS layer can be used to facilitate grid recovery from tissue culture plasticware.

We have tested the 3D printed holders with little success in our lab. Accordingly, we cannot recommend it. The PDMS layer is a great suggestion and we've added it (including the reference from above).

9) Line 114: "Fiducials should be chosen both in size and brightness to be compatible". Please specify which beads (company and material numbers) are recommended.

According to JOVE guidelines, brand names etc. should not be present in the main text. We provide bead vendors (1 µm) in the materials xls file. Concentrations are provided in the main text.

10) Line 117-119: Statement: "…do not use beads too bright…" Please be more specific.

We've added a respective comment.

11) Line 137: Please specify how to judge optimal blotting time.

As requested, a comment has been added.

12) Line 145: Autogrids without cutouts are suboptimal and should not be recommended here.

We agree that this might be confusing to newcomers and we now only suggest cutout-autogrids. However, we still successfully use regular autogrids on occasion ...

13) Lines 143-169: Section 2 "Cryo-Fluorescence Light Microscopy" is missing many important details. Please provide settings for Z-stack sampling, NA, and magnification of the objective, if confocal or wide-field imaging was used. Please provide the X-Y, Z-

theoretical Nyquist resolution. This is very important for others to know to judge whether their system is suitable for the protocol.

Details have been added to the text and the “Settings” tab of the Materials .xls

14) Lines 174-222; Section 3 "Focused Ion Beam Milling" is again missing many details. This section is most crucial for the complete workflow and needs to be completely revised. Please provide a separate section with a detailed description of how the correlation and transfer of positions are done. Describe how to use 3DCT software using detailed figures describing step by step how this is performed. While this may be captured on the JoVE video later, there should be also a detailed written protocol available. The 3DCT seems to be a major advancement since Arnold et al. publication, yet it is not well explained here and many reader, buts may not be aware of it.

We have added a more detailed explanation to our text and also point out the online tutorial for 3DCT. The figures have been updated and improved as well.

15) Line 203: Note. The fact that fine milling must be done immediately after rough milling is limiting the number of lamellae that can be prepared due to ice deposition on polished lamellae. How many lamellae are recommended per session?

There is no definitive answer for that. It appears that all (TFS) FIB/SEM systems show slightly different recontamination rates (< 50 nm/h is “within specs”). We now try to explain this concept in more detail to allow users to make an educated decision on the exact number of lamellas that can be cut. But this needs to be up to the user and how fast they are ...

16) Line 205: "…or by using scripting…" The transfer of the milling position is the most crucial step for the precision of the targeted milling. A "manual" transfer of the position is certainly not precise enough to target any individual cellular structures. Please provide the code of the mentioned script and describe in detail the exact procedure.

Manual transfer in fact is precise enough (given precise enough measurements) and was used for the “Representative Results” here. However, automated transfer is of course preferable. We now also cite SerialFIB, which contains functionality to transfer positions from 3DCT to the FIB.

17) Line 206: Please add the missing reference for stress relief cuts (doi.org/10.1016/j.jsb.2019.09.006).

The reference has been added.

18) Line 213: "…generally thought to reduce data quality…". Please provide a reference for this statement.

We explain this now in more detail. Thicker samples correspond to more electron scattering events. A sample should therefore be thin and only consist of the material of interest, i.e. the cellular lamella. Recontamination adds unwanted, amorphous ice to both sides of the lamella. For an Aquilos1 for example, up to 50 nm/h is still considered “within specs”! This unwanted material of course will cause unwanted scattering events and hence deteriorate the signal.

19) Line 219; Section 3.6. Please provide more details on the evaluation of the accuracy of milling. What should one do in case the lamella is bent or has moved and how can one recognize that this has not caused that the FM signal is not anymore preciously corresponding to the initial coordinates?

We’ve added a comment, that users should regularly check for such movements. If it becomes too excessive (>300 nm), the site should be discarded as the correlation will be out of registration. A potential solution, i.e. integrated FLM setups, is also pointed out.

20) Lines 226-241; Section 4 "Correlative TEM": Please provide more details on how this step is performed. Especially Step 3.4 is essential for successful targeting and is not described well with essential information missing. Please add detailed step-by-step instructions on how this correlation is performed. Is the correlation done in SerialEM, in MAPS, or another software? A figure describing this step is necessary, as it is together with step 3.3 the most crucial step for the correlation.

Details have been added and are now supported with a dedicated figure.

21) Line 244: "While we have successfully applied this protocol to a variety of different samples" Please provide all references for the different samples on which the workflow was applied.

Our protocol in fact summarizes our experience on three different published target structures: lipid droplets (Arnold et al.), the END, and autophagic bodies (containing END) removed by autophagy (Wilfling et al.). There are several more pending for publication, including autophagy intermediates in yeast and mammalian cells, LLPS compartments involved in B-cell priming, and centrosomes just to name a few.

Obviously, they cannot be revealed at this point. The statement has been adjusted to account for that.
As a community service, however, we would like to make our experience available to other labs now.

22) Line 245-246: "…we here provide a walkthrough of the pipeline that was used in the discovery of the Ede1-dependent endocytic protein deposit (END) in S. cerevisiae." Please add the missing reference to the publication on which your representative results are based: Wilfling et al., 2020, doi.org/10.1016/j.molcel.2020.10.030

The reference has been added.

23) Line 255: "FLM stack acquisition" Please provide details on the used microscopy system.

Details have been added to the resource file.

24) Lines 269-270: "Since the correlation was found to be accurate.." Please describe how accuracy was determined and which accuracy exactly was measured. This is essential to evaluate the precision of the here described targeted milling.

The details on how accuracy can be judged have been provided in the protocol and discussion section.

25) Line 288: "Overall, a correlation success of ~75% was achieved" Please describe how the correlation success was defined and quantified. Please provide all correlation examples for this analysis.

Correlation success is defined as correlated lamellas that survived transfer to the TEM and sowed the END compartment. It is hardly possible to show all the positions that have been processed within the scope of this (video) protocol. We've added the total numbers (12 milled lamellas, 9 END structures found) to the statement.

26) Line 340, Figure 8: Please provide an actual correlated image of the FLM and TEM image in addition to the red cross which only indicates where the fluorescent signal is supposed to be.

The classical CLEM view has been added (Fig. 7B).

27) Line 356: "In this regard, testing different denoising or deconvolution techniques on the FLM data is also advised, as it may considerably improve the localization of fiducials and cellular signals.". Please provide references for denoising and deconvolution techniques suitable for cryo samples.

References for algorithms that can be used for deconvolution are provided (e.g. Huigens). But since there's nothing special about cryo-FLM data, any algorithm that works at RT should also be applicable to cryo-conditions. We now also cite Florian Jug's N2V.

28) Lines 392-401, Section 3 "Limitations of the method": Please make clear that this approach is sensitive to lamellae movement during milling in respect to the fiducial markers. In addition, it should be mentioned that fine milling should be performed immediately after the rough milling of each lamella. In such a case, the throughput is limited to few lamellae or it leads to increased ice contamination which is detrimental for subsequent cryo-ET.

We've added more discussion and suggestions regarding this topic in both the protocol and the discussion section. We also do recommend the site-wise approach. This however still allows experienced users to finish ~4-6 lamellas in a time-frame compatible with the recontamination rates of the FIB/SEMs.

Reviewer #2:

Manuscript Summary:

This manuscript provides a step-by-step protocol of a cryo-correlative microscopy workflow for 3D localisation of fluorescent signals in cells that are thinned by cryo-FIB milling and imaged by cryo-ET. Such a detailed description comes very timely as these methods are gaining popularity while they still require significant expert know-how. While for cryo-FIB milling and cryo-ET of cells, a number of good methodological papers are available, the practical aspects of how to use 3D correlative microscopy to prepare lamellae in a targeted fashion by precisely locating fluorescent signals during the milling process have been missing. The authors use the example of aberrant yeast endocytic sites which they and others have previously described to be autophagy-precursors and liquid-liquid phase separation events (Wilfling et al Mol Cell 2020, Kozak & Kaksonen, bioRxiv 2019).

While I support the publication of such a protocol article, I think the authors could improve the manuscript in multiple ways to make it a more helpful resource. Here's my suggestions for improvements, as well as some needed clarifications.

Major Concerns:
- As the correlative part is the central advance presented in this paper, the correlation procedures used should be most extensively explained. The descriptions of the correlation procedures (performed at multiple steps) do not contain sufficient details to be useful. This relates to all steps at which correlations between image modalities are done. It would also be good to explain whether and why certain software or algorithms are better for 2D or 3D correlations. Further example, in point 3.3 of the protocol and legend to Fig 4: what is 3DCT? If this is the preferred software, then it may be helpful to use it as a paradigm to describe the procedures in more detail.

As suggested, we now discuss the 3D correlation toolbox (3DCT; Arnold et al.) in more detail and point out an online walkthrough of its features and use.

- line 61- 62: The statement 'Ensure that sites of interest can be localized successfully with a good signal to noise ratio at room temperature in a fluorescence microscope' is very vague. What is a good signal to noise ratio? Can the authors provide some estimate? And what configuration of a fluorescence microscope is meant?

We now provide details on the microscopes and their settings (see Materials.xls). There is no estimate on the exact SNR that can be useful. We've changed the statement to rather alert the reader of the (obvious) fact that the signal of interest needs to stand out above background (in cryo!).

- line 67: In what respect did mVenus perform better than EGFP? This is again a vague and therefore not helpful statement.i

The hypsochromic shift is now discussed and why it may be useful for standard filter combinations. mVenus is also ~1.6x brighter than EGFP (ref. 25 in text) and hence leads to higher photon count and ultimately higher localization accuracy. [This note has been moved to discussion section]

- line 68-69: I do not think the sentence regarding trade-off between wavelength and localisation accuracy with reference to Abbe's diffraction limit makes sense. For the localisation precision of point sources (as are fiducials and the majority of signals dealt with here), Abbe's law is not limiting. The emission wavelength of the fluorophore can almost certainly be neglected for the localisation accuracy in CLEM. However, what does matter is the numerical aperture of the objective, because the number of collected photons (and hence the sensitivity) depends on it.

This conceptual issue seems to also be reflected in lines 117 -118: The localisation limits of conventional FLMs are at least one magnitude smaller than the size of beads of 0.5-1 µm, so I don't understand this statement. Beads of diffraction-limited size (like 50 nm or 100 nm) can be localised equally well - it is a matter of detectability and number of emitted and detected photons, not size.

It is true that the Abbe diffraction limit is not (the only) limiting factor here. This has been corrected and is now discussed in more detail. [This note has been moved to discussion section]

- line 88-89 and lien 355: What is an 'optimal' dilution of fiducial markers? Also, fiducial markers are mentioned early on in the protocol, without really explaining their purpose, which would make it easier to assess what is meant by optimal.

When we now introduce fiducial markers, we also provide more details on their function and optimal properties.

- line 107: Reference(s) for grid patterning protocols should be added.

We now cite the grid patterning protocol.

- line 111: Why are metal oxide grids mentioned? What would be their purpose? This mention comes out of the blue and it's not clear why.

This was indeed too vague and due to JOVE's instructions to not provide brand names in the main text. This has now been corrected and should be clear now.

- line 131: In fact to minimise contaminations it would be better to perform steps in the gas phase a few centimetres above the liquid phase of lN2, not in the liquid phase.

This seems to be a matter for debate and maybe "culture" of lab. To our knowledge, there is no literature showing that one way is significantly better than the other. In our hands, working in the liquid has worked well so far - at least for beginners. It may be true, however, that with experience (and steady hands) working in the gas phase is better.

- line 160-161, and Figure legend 3: Although convolution is mentioned in the text and shown in Fig 3, an explanation of what is actually done and why it would be beneficial for the CLEM procedure is missing. In particular the panels with graphs and analysis shown in Fig 3 are not explained at all in the legend. Also, the legend

does not say whether the red signals in Fig 3 are fiducials or signals of interest.

Deconvolution and its benefits are now better discussed. Fig. 3 and its legend have been updated.

- line 165-166: Why check for bleed through? In some cases (fiducial markers) bleed through is desirable because it allows to align channels to each other and correct for chromatic aberration.

This has been updated. We now describe why too much bleed-through would be problematic. We've added a comment regarding chromatic aberration.

- line 199-200, line 268 and line 364: accuracy of correlation is mentioned in several instances. However, the authors give no estimate for the accuracy in their example / proof of principle. Also, how dependent is the accuracy of locating the position of the lamella in z on the z-distribution of the fiducials? It would be good to get some estimates or ideas on that, or even better some actual measurements.

We've added a statement on the z-distribution of fiducial beads and that it is indeed beneficial to have a nice z-distribution. A detailed description on the accuracy of the method is available in Arnold. et al. However, we here provide some practical (rough) guidelines on the RMSE values and how to judge (e.g. base on fiducial beads not used for registration) if the correlation is trustworthy or not.

- line 217: Is bending / deformation really such a problem for correlation? If lamellae are bent by dimensions that are similar to correlation accuracy (which I guess is in the hundreds nm range), then they are too deteriorated for high-quality cryo-ET anyway. Deformations that are harmless to cryo-ET are likely to be neglectable for correlation. However, as the authors do not provide an estimate for the correlation accuracy in z, it remains difficult to assess.

We now mention the accuracy on the IB image also derived in Arnold et al., which is ~ 300 nm. This is in fact a combination of x,y, and z due to the tilted IB image with respect to the FLM stack. It is certainly true that lamellas that exceed this value should be discarded because they are too deteriorated. We now instruct the users to regularly check for such movement/bending and to discard the site if bending > 300 nm is detected.

- It may make more sense to swap the order of Fig 4 and 5.

The order of the figures has been revised.

- legend Fig 5: At this stage of the pipeline, the grid is already in the FIB microscope. So how can the title be 'finding suitable grid squares for FLM stack acquisition'? The figure shows steps after FLM.

The legend has been updated.

- legend Fig 8, line 340-341: 'can readily be correlated': How exactly? It may be obvious to the authors but to the reader, this is not helpful.

The details are now provided in the text.

- line 397: The use of stained lipid droplets as fiducials is mentioned. The relevant paper should be cited (Scher N. et al, bioRxiv 2021)

The citation has been added.

Minor Concerns:

- The summary says 'Proteins of interest (POIs) are fluorescently tagged, their 3D position …' the manuscript however does not describe fluorescent tagging of proteins. This should be modified.

This has been corrected.

- In the abstract, the phrasing doesn't make clear that FIB milling is the solution to thinning samples and thus making them amenable to cryo-ET.

This has been adjusted.

- line 74: 'stable are handled' should probably read 'stable and handled'

This has been fixed.

- line 77: By grid hole size, do the authors mean 'grid square size' or (carbon or SiO2) 'film hole size'?

This has been fixed.

- line 116: 'channel the biological' should probably read 'channel than the biological'

This has been fixed.

- line 179: What does 'as required by the system' mean?

What we meant to say was “depending on which TEM is available”. We’ve rephrased the sentence.

- line 214: 'two-step fashion: first rough, then fine': It is not clear that the authors mean first ALL lamellae are milled roughly, then ALL are milled finely (in contrast to each lamella is milled roughly as well as finely before proceeding to the next lamellae, as they then go on to suggest). This needs to be more clearly phrased.

This has been rephrased as suggested.

- line 229: be more precise what is meant by 'lamella orientation'. It is not clear from this sentence HOW it should be orientated. Perhaps refer to figure, that could help.

This has been updated and is now also illustrated more clearly by Fig. 2.

- line 231: by 'lamella square', do the authors mean 'lamella-containing grid square'?

This has been updated.

- The paragraph introducing Ede1 should cite the relevant literature.

The paper is now cited.

- Line 288: What does 'correlation success of 75%' mean? Does it mean that 75% of targeted spots could be correlated to similar structures found in cryo-ET? Or does it mean that 75% of spots identified by cryo-FM could be located to lamella?

We define as success the number of lamellas that survived milling and loading into the TEM and that contained END structures (9) vs. the total number of lamellas cut (12). This is now explained in the text.

- Figure legend 2: Does the Figure show HeLa cells? It should be specified in each legend what is shown in the figure, especially if it is not yeast cells which are the proof-of-principle in the manuscript.

Even though the protocol is compatible (and has at this point been tested on a variety of cells; several unpublished), we now choose to only show yeast cells as to make the entire protocol more consistent.

Editorial comments:

Changes to be made by the Author(s):

1. Please take this opportunity to thoroughly proofread the manuscript to ensure that there are no spelling or grammar issues.

We did our best to check for spelling and grammar issues.

2. Please provide an email address for each author.

Email addresses for each author have been added.

3. Please rephrase the Summary to clearly describe the protocol and its applications in complete sentences between 10-50 words: “Here, we present a protocol to …”

The summary has been rephrased.

4. Please remove the citations from the Abstract and include them in the Introduction section.

We’ve removed all citations from the abstract.

5. Please ensure that abbreviations are defined at first usage.

Abbreviations should now always be defined upon first use.

6. JoVE cannot publish manuscripts containing commercial language. This includes trademark symbols (™), registered symbols (®), and company names before an instrument or reagent. Please remove all commercial language from your manuscript and use generic terms instead. All commercial products should be sufficiently referenced in the Table of Materials. Please sort the Materials Table alphabetically by the name of the material.

Commercial language has been removed. Materials are listed in alphabetical order.

7. The Protocol should be made up almost entirely of discrete steps without large paragraphs of text between sections. Please simplify the Protocol so that individual steps contain only 2-3 actions per step and a maximum of 4 sentences per step.

We've updated the protocol as suggested.

8. Please ensure that all text in the protocol section is written in the imperative tense as if telling someone how to do the technique (e.g., "Do this," "Ensure that," etc.). The actions should be described in the imperative tense in complete sentences wherever possible. Avoid usage of phrases such as "could be," "should be," and "would be" throughout the Protocol.

Any text that cannot be written in the imperative tense may be added as a "Note." However, notes should be concise and used sparingly, and also one Protocol step cannot have multiple notes. Please consider moving some of the notes about the protocol to the discussion section.

We've updated the protocol as suggested. Where possible, "Notes" have been moved to the discussion section.

9. Please note that your protocol will be used to generate the script for the video and must contain everything that you would like shown in the video. Please ensure you answer the "how" question, i.e., how is the step performed? Alternatively, add references to published material specifying how to perform the protocol action. There should be enough detail in each step to supplement the actions seen in the video so that viewers can easily replicate the protocol.

We've added more details so that each step is self-explanatory.

10. Please add more details to your protocol steps.

We have added details as also discussed above.

Line 86: what is meant by "any treatment" here? Again, please avoid generic statements in the Protocol step.

As treatments will HIGHLY depend on the biological system targeted by our 3D-correlative FIB approach, a generic term appears to be necessary here. We however now provide examples.

Line 94: Please mention the concentration of the cleaning compounds used and also briefly the cleaning procedure.

We here refer to plasma cleaning (i.e. no reagents). Settings for our instrument are now provided in the Materials xls.

Line 98: Please specify the centrifugation speed and temperature.

Since for some beads the procedure may differ, we have changed this sentence and now refer to the manufacturer's instructions (e.g. dialysis vs. centrifugation).

Step 1.3: Please provide the action steps as discrete steps. Rest can be moved to the Discussion part.

The section has been revised. Note has been moved to the discussion section.

Step 2.4/4.3: Please provide more details if this step needs to be filmed.

2.4 is now 2.3. As deconvolution should be a general enough concept, it doesn't need to specifically be filmed here.
By referencing earlier steps and providing some more detail (including also an improved figure), 4.3 should now be better explained, sufficient for filming.

Line 176: Please mention how to take the note on orientation.

This has been updated and should now be better explained in text and using Fig. 2A

Line 179: What organometallic and conductive layers to be applied? Please specify the amount and concentration.

Details are now provided. Settings are summarized in the Materials xls.

Step 3.2: Please provide more details if this step is to be filmed. Also, please see if the angle can be specified here.

Details are now provided.

Line 193: Please define the term IB.

Ion beam (IB) is now defined in 3.4 upon first use.

11. In the software, please ensure that all button clicks and user inputs are provided throughout.

We now also point out button clicks. Additionally, we reference a walk-through that explains individual buttons in 3DCT and their use.

12. Line 245: Please define Ede-1.

EH domain-containing and endocytosis protein 1 (Ede1) is now defined.

13. Line 388: Please define CLEM.

Correlative light and electron microscopy (CLEM) is now defined (line 59).

14. Please sub-number the Figures as (A), (B), (C), etc., where multiple panel figures are there.

Panel figures are now sub-divided in A), B), C) etc.

15. Figure 3: Please ensure that the description of the xy-axis is clearly visible in the graphical representations.

We've added the necessary labels to the axes.

16. Please remove the DOI numbers from the References

DOIs have been removed.